Color transparency in hadronic attenuation of ρ^0 mesons

K. Gallmeister, M. Kaskulov, and U. Mosel
Institut für Theoretische Physik, Universität Giessen, Germany
(Dated: November 12, 2010)

Ongoing experiments at JLAB investigate the nuclear transparency in exclusive $\rho^0(770)$ electroproduction off nuclei. In this work we present transport model predictions for the attenuation of ρ^0s in nuclei and for color transparency (CT) effects as observable at CLAS with a 5 GeV electron beam energy. A full event simulation developed here permits to study the impact of actual experimental acceptance conditions and kinematical cuts. The exclusive $(e, e'\rho^0)$ cross section off nucleons is described by diffractive and color string breaking mechanisms extended toward the onset of the deep inelastic regime. Different hadronization and CT scenarios are compared. We show that a detailed analysis of elementary cross section, nuclear effects and experimental cuts is needed to reveal the early onset of ρ-CT at present JLAB energies.

PACS numbers: 13.75.-n, 13.85.-t, 25.40.-h, 25.80.-e

I. INTRODUCTION

Electroproduction experiments of hadrons on nuclear targets may offer a chance to observe the effect of color transparency (CT), that is the phenomenon of vanishing (or very small) final state interaction (FSI) of the produced hadron with the surrounding nucleons, at high momentum transfer [1–5]. The HERMES experiment at DESY [6] (see [7–9] for other experiments at higher energies) looked for such an effect in the electroproduction of ρ^0 mesons on nuclei. While a rise of the transparency T_A[1] with photon virtuality Q^2 was indeed observed and taken as evidence of a ρ-CT effect other studies showed that the same data could be well understood in a sophisticated transport calculation [10] or even a Glauber calculation [11]. In these studies the observed rise of T_A was attributed to the change of the coherence length, i.e. to the Q^2-dependence of shadowing in the entrance channel. The observation of ρ-CT, therefore, demands a kinematical regime where one is less sensitive to the resolved hadronic interactions of the incoming photons. A new experiment at JLAB has been designed to work under kinematical conditions that keep the coherence length small and nearly constant [12]. It is supposed that in this case a rise of T_A as a function of Q^2 should indeed indicate an onset of CT.

In Ref. [13] first theoretical estimates have been made for the expected results. The framework used is essentially a Glauber calculation, with the prehadronic interactions being described by the pQCD-inspired cross section of Farrar et al. [5]. In this model the prehadronic cross section consists of a $1/Q^2$-dependent starting value; the cross section then increases linearly in time up to an expansion time where it reaches the full hadron-nucleon cross section. The result of Ref. [13] was a transparency ratio T_A strongly rising with Q^2.

The main scope of Ref. [13] was a description of FSI only. The elementary reaction process played no role, i.e. all the ρ mesons produced experience CT, independent of their production mechanism. However, as we will demonstrate in this paper, the knowledge of the elementary exclusive cross section $(e, e'\rho^0)$ off protons *and* neutrons is a necessary prerequisite for a proper description of the transparency ratio T_A and thus a proof of the CT effect.

In addition, in any analysis of CT it is essential to account for the experimental acceptance limitations [10]. So far, the acceptance conditions applied in the JLAB experiment and the interplay of kinematical cuts with standard nuclear effects like Fermi motion and FSI of ρ^0 and its $\pi^+\pi^-$ decay products have not been studied. We will show that the experimental cuts may strongly affect the transparency ratio and produce at high values of Q^2 a behavior which may overshadow and/or mimic the rise of T_A.

In the following we study the ρ^0 production on ^{12}C and ^{56}Fe nuclei. We choose the kinematical conditions for our calculations such that they correspond as nearly as possible to the actual values of the ongoing experiment at JLAB [12]. In particular we look for the region at smaller Q^2 where the experimental values are centered and discuss also the event-types and $\rho^0 \to \pi^+\pi^-$ reconstruction problems in this experiment. The main focus of our studies is to clarify the observable consequences of CT effect and investigate possible other effects that might influense the wanted ρ-CT signal. Such an analysis of CT at present JLAB energies is challenging due to the combined contribution of different effects such as the uncorrelated $\pi^+\pi^-$ background affecting the $\rho^0 \to \pi^+\pi^-$ signal, the largely reduced (by experimental cuts) phase space, nuclear FSI and Fermi motion effects.

The outline of the present paper is as follows. In Sec. II we describe the model used in the calculation of exclusive $(e, e'\rho^0)$ cross section of nucleons. In Sec. III we introduce the GiBUU model used in the calculations and also describe the hadronization and CT scenarios followed in this work. The experimental cuts used in the experiment

[1] The nuclear transparency for a certain reaction process is usually defined as the ratio of the nuclear cross section per target nucleon to the one for a free nucleon, i.e. $T_A = \sigma_A/A\sigma_N$.

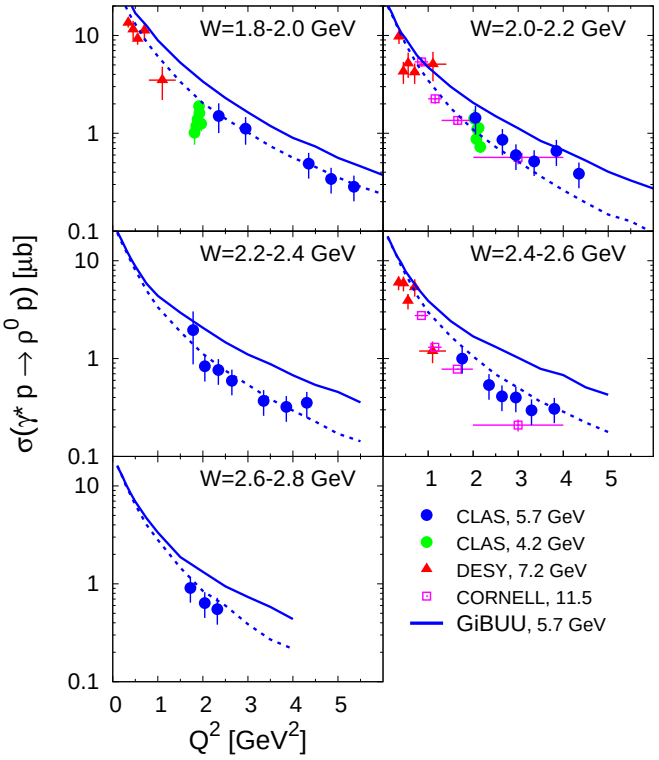

FIG. 1. (Color online) Q^2 dependence of the integrated cross section in the reaction $p(\gamma^*, \rho^0)p$ (solid curves) for different W bins above the resonance region. The compilation of experimental data is taken from Ref. [23]. The dashed curves describe the corresponding cross sections in the reaction $n(\gamma^*, \rho^0)n$.

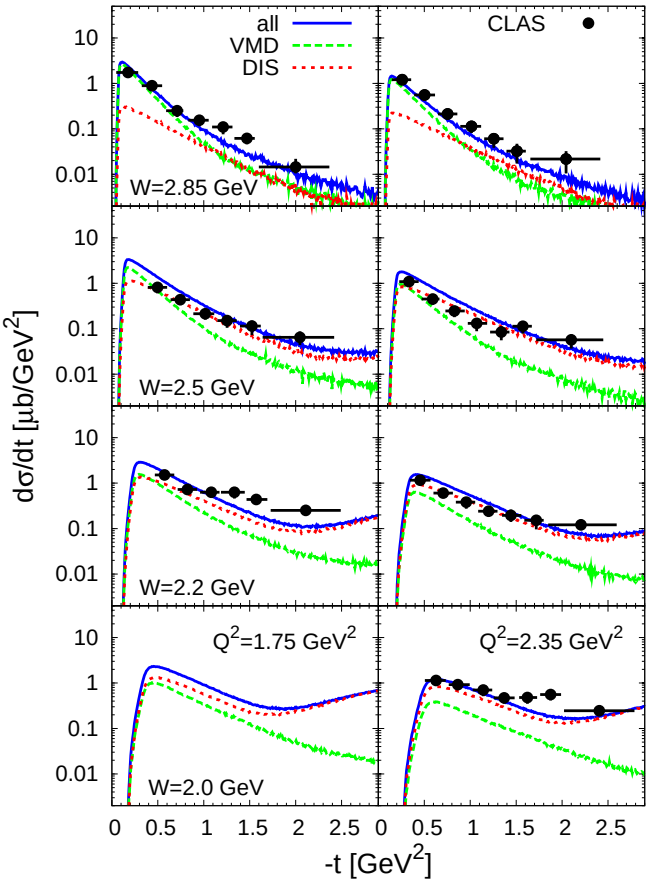

FIG. 2. (Color online) Differential cross section $\mathrm{d}\sigma/\mathrm{d}t$ in the reaction $p(\gamma^*, \rho)p$ for different (W, Q^2) bins. The experimental data are from Ref. [23]. The solid curves are the sum of VMD (dashed) and DIS (dotted) contributions.

at JLAB are considered in Sec. IV. The effect of Fermi motion in the transparency ratio is discussed in Sec. V. The results are presented in Sec. VI. The conclusions are summarized in Sec. VII.

II. EXCLUSIVE $\rho^0(770)$ PRODUCTION

The exclusive production of mesons may involve very different production mechanisms driven either by hadronic or by hard partonic interactions. The CT occurs in the scattering of virtual photons off partons. Indeed, in Ref. [14] it was shown that the exclusive π^+ electroproduction and the CT signal observed in this reaction off nuclei [15–17] can be understood if only the hard partonic events [18, 19], that go through high-lying excitations of the nucleon [20], experience an expansion time and a corresponding CT effect. In analogy, the unambiguous identification of the ρ-CT effect requires the understanding of the elementary ρ^0 production mechanism. Also the elementary cross sections off nucleons are the first input in any event generator attempting to describe the corresponding reaction off nuclei. We are interested in the description of exclusive ρ^0 production around the values of $W \simeq 1.8 \ldots 2.8\,\mathrm{GeV}$. This is very difficult task because in this region the contributions of large amount of nucleon excitations should be accounted for explicitely, see Ref. [21] and references therein.

To account for the contribution of nucleon resonances we consider the DIS like interaction with partons since DIS involves the excitation of all possible resonances. To validate this assumption the high energy event generator PYTHIA is used that – besides diffractive vector meson dominance (VMD) events – also describes hard scattering events in a string-fragmentation picture. In PYTHIA the exclusive ρ^0 production is treated as exclusive limit, $z \to 1$, of semi-inclusive DIS

$$p(e, e'\rho^0)X \longrightarrow p(e, e'\rho^0)p \quad \text{for} \quad z \to 1. \qquad (1)$$

This is in the spirit of the exclusive-inclusive connection [22].

However, it is not obvious that the event generator designed for inclusive reactions should also work in exclusive processes. In Figure 1 we, therefore, show the results for the Q^2 dependence of the integrated cross section for the exclusive reaction $p(\gamma^*, \rho^0)p$ above the resonance re-

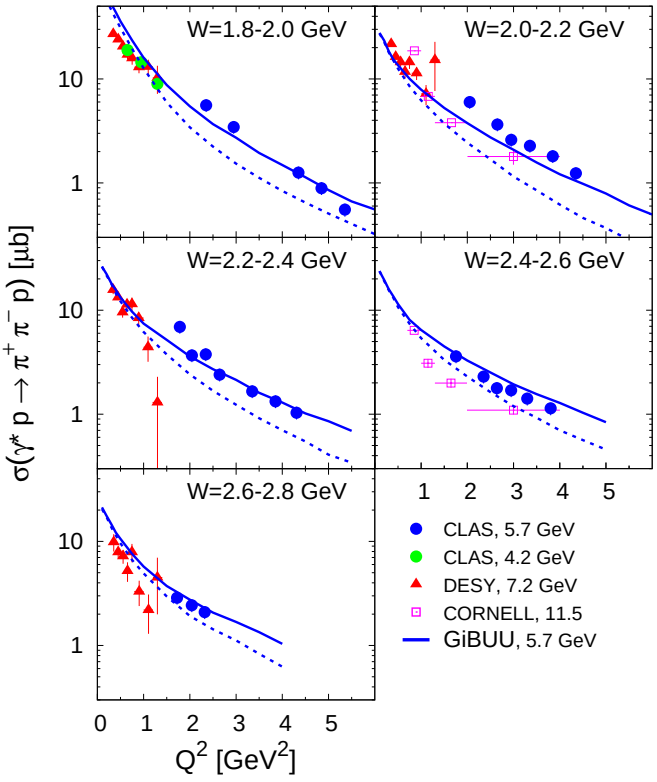

FIG. 3. (Color online) Q^2 dependence of the integrated cross section in the reaction $p(\gamma^*, \pi^+\pi^-)p$ (solid curves) for different W bins. The compilation of experimental data is taken from Ref. [23]. The dashed curves describe the corresponding cross sections in the reaction $n(\gamma^*, \pi^+\pi^-)n$.

gion. The Q^2 range shown there is the one covered by the JLAB ρ-CT experiment. The curves correspond to the default parameters used in the PYTHIA generator.

The Pomeron induced diffractive production of ρ^0 is isoscalar in nature. On the contrary the DIS production of ρ^0 introduces an isospin dependent component which makes the cross sections off protons and neutrons unequal. Therefore, we also show in Figure 1 the production of ρ^0 in the reaction $n(\gamma^*, \rho^0)n$ off neutrons. The isospin dependence of the ρ^0 production cross section and its contribution to T_A have not been considered before; the naive assumption $\sigma_p = \sigma_n$ was always used. The latter has important consequences in isospin asymmetric systems such as the ^{56}Fe nucleus studied at JLAB. Note that in the JLAB experiment the transparency ratio T_A is normalized to the cross section on the deuterium target.

In Figure 2 we show a comparison of the differential cross section $\mathrm{d}\sigma/\mathrm{d}t$ in the exclusive reaction $p(\gamma^*, \rho^0)p$ with the experimental data from Ref. [23]; the contributions of DIS and diffractive VMD events are given separately. The PYTHIA model describes the magnitude and the shape of the differential spectra very well.

In Fig. 2 it can also be seen that in the region $W \simeq 2$ GeV the DIS mechanism gives the dominant contribution whereas at higher values of W the diffractive VMD component dominates the forward production of ρ^0. Concerning the Q^2 dependence the region of low Q^2 is always dominated by the VMD events (see discussion below). At large values of Q^2, however, the VMD component is strongly decreasing and the ρ^0 production mechanism in the forward and off-forward regions is driven by the partonic DIS component. Because in DIS the deep inelastic structure function is factorized out of the fragmentation function the Q^2 dependence of the transverse cross section in $p(e, e'\rho^0)p$ must essentially follow the Q^2 dependence of the total DIS cross section. This behavior has been already observed in exclusive π^+ electroproduction [18]. We find here that the situation is similar in exclusive ρ^0 production and that the ρ^0 experimental data follow this behavior as well.

Interestingly, the Lund Model used here for the hadronization predicts two jets for the $\rho^0 p$ final state in the forward and backward directions. Therefore, there is a sizable backward production of the ρ^0. In the experimental analysis of Ref. [23] the off-forward region is extrapolated by assuming a functional form as e^{bt} thus missing the backward rise. Since, the backward production of ρ^0 is large and has been not taken into account in [23] the data may underestimate the actual integrated cross section. This can be seen by comparing Figure 1 and Figure 2 where the forward angle data are consistent with the model while the integrated cross sections are consistently lower than the model at higher values of Q^2.

In the actual experiment the ρ^0 is reconstructed from its $\pi^+\pi^-$ decay products. Therefore, one has to also control the uncorrelated $\pi^+\pi^-$ background which may contaminate the ρ^0 signal. The same string fragmentation picture is applied to the uncorrelated $\pi^+\pi^-$ background as implemented in the PYTHIA generator. In Figure 3 we show the Q^2 dependence of the integrated cross sections in the reaction $p(e, e'\pi^+\pi^-)p$ off protons. The compilation of experimental data is from Ref. [23]. They include the correlated $\rho \to \pi^+\pi^-$ as well as the uncorrelated $\pi^+\pi^-$ events. The two basic mechanisms, diffractive production and hard DIS production, together describe the data very well.

Since the experimental cuts do not allow for a perfect separation of diffractive events, we show in Figure 4 the relative importance of diffractive VMD and DIS events over the full sample. We show the result for deuterium D as an example, but the conclusions are valid also for other nuclei, except for the kinematical limitations at high Q^2. FSIs do not affect the relative importance of the production mechanisms, but they do affect the relative importance of the two components in the observed sample.

The relative importance of the two event types depends strongly on whether we count all reconstructed ρ^0 or only those, which are real ρ^0. In DIS events the probability of reconstructing a ρ^0, which is indeed a fake one, is much larger than in VMD events. As one can see in

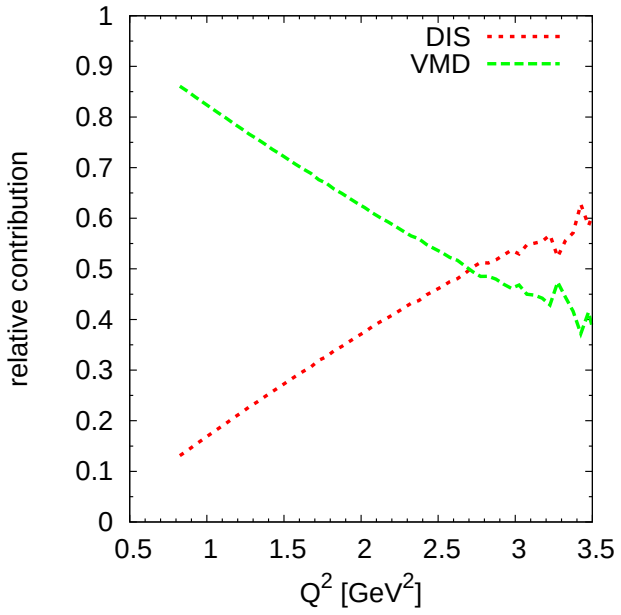

FIG. 4. (Color online) The relative importance of VMD (green dashed) or DIS (red dotted) events compared to the total sample as function of Q^2 for D target. Only real ρ^0 are selected, there are no fake reconstructions.

Figure 4, already in an experiment, which can distinguish between 'true' and 'fake' ρ^0 mesons, the DIS component is non-negligible over the full Q^2 range, increases strongly with Q^2 and becomes even dominant for the values of $Q^2 \gtrsim 2.5\,\mathrm{GeV}^2$. For the actual experiment, where the fake and the true ρ^0 mesons cannot be distinguished, this transition happens even earlier (see Fig. 2).

III. CT IN THE TRANSPORT OF ρ^0 IN NUCLEI

The theoretical framework followed here is the GiBUU transport model [24]. In this model first the primary interaction of the incoming electron with the nucleons of the target nucleus is described within the impulse approximation; the latter assumes that the interaction takes place with only one nucleon at a time and is expected to be valid for the momentum transfers treated here. Fermi distribution of nucleons follows the local density approximation.

The fate of produced hadrons in FSI is then described by the coupled-channel Boltzmann-Uehling-Uhlenbeck (BUU) transport equation which describes the time evolution of the phase space density $f_i(\vec{r},\vec{p},t)$ of particles of type i. Besides the nucleons these particles involve the baryonic resonances and mesons that can be produced in FSI. For the baryons the equation contains a mean field potential which depends on the particle position and momentum. The BUU equations of each particle species i are coupled via the mean field and the collision integral. The latter allows for elastic and inelastic rescattering and side-feeding through coupled-channel effects; it accounts for the creation and annihilation of particles of type i in a secondary collisions as well as elastic scattering from one position in phase space into another. The resulting system of coupled differential–integral equations is solved via a test particle ansatz for the phase space density. For fermions Pauli blocking is taken into account via blocking factors in the collision term. The model has been widely tested and validated for very different types of reactions, from heavy-ion over hadron-induced reactions up to electron- and neutrino-induced reactions on nuclei. All the details about the GiBUU code and the comprehensive list of publications describing the model can be found in [24].

In electroproduction, the ρ^0 mesons are reconstructed from $\pi^+\pi^-$ pairs, both in the actual experiment as well as in our simulations. Therefore, for realistic calculations, it is important to account for the in-medium decay and attenuation of $\rho^0 \to \pi^+\pi^-$ decay pions. These pions, after the ρ^0 decay inside a nucleus, propagate further through the nucleus and experience FSI. Thus, the final result, T_A, is not only affected by ρ^0 absorption, but also by pion FSI. The most striking result of our studies is the large effect of the pion interactions: half of the observed attenuation is due to pion absorption. Since the effect of the pionic interactions is so large, it is not appropriate to distinguish between absorption of the ρ^0 and some 'small' [13] pion absorption correction. Instead it is necessary to use a model, like the one used here, which is capable of treating all the particle species and their interactions consistently.

There is no definite framework to accommodate the notion of CT in theoretical models. Different CT scenarios exist in the literature. For example, in Ref. [25, 26] a color dipole model has been applied to high-energy reactions in which all the hadronization happens outside the target nucleus. In the present model, aimed at the description of experiments in a kinematical regime where hadronization mostly happens inside the nuclear target, we use the concept of *production* and *formation* times for production of a 'constituent' quark and formation of a color-neutral hadron as developed in [27].

The prehadronic interactions between the production time and the formation time follow the pQCD-inspired quantum diffusion model of Ref. [5] assuming that the formation time corresponds to the expansion time of a point-like configuration (PLC). In this picture the cross section in FSI grows linearly with time τ [5]

$$\sigma_{\mathrm{eff}}(Q^2,\tau) = \sigma_{\mathrm{tot}} \times \left[\left(\frac{r_{\mathrm{lead}}}{Q^2}\left(1-\frac{\tau}{\tau_f}\right)+\frac{\tau}{\tau_f}\right)\Theta(\tau_f-\tau)+\Theta(\tau-\tau_f)\right] \quad (2)$$

where r_{lead} is the ratio of leading quarks to all quarks in the hadron. The scaling with r_{lead} guarantees that summing over all particles in an event, on average the prefactor becomes unity. In the presence of the CT effect, see the factor $\sim 1/Q^2$ in Eq. (2), the intranuclear

attenuation of hadrons propagating through the nuclear medium decrease as a function of photon virtuality Q^2.

The hard part of the primary high energy electromagnetic interaction is described by the Lund model which means that the final state consists of an excited string. This string then fragments into hadrons. An extraction of the *formation* time τ_f in the target rest frame follows the space-time pattern of hadronization as described in Ref. [27]. This model has been already successfully applied to the hadron attenuation experiments at 200-280 GeV (EMC), at 28 GeV (HERMES) and at 5 GeV (JLAB) [14, 28].

In our earlier studies of the π-CT experiment [14] we had argued that only the DIS events should experience CT. For ρ^0 production the situation might be, however, different for the diffractive process. Now the incoming photon can fluctuate into a resolved ρ^0 component. Experiments could thus be influenced also by the prehadronic formation and expansion period of this diffractively produced ρ^0 mesons. It is, therefore, of interest to study the relative importance of DIS to diffractive events. Such a distinction could give valuable information on the mechanism of CT. Therefore, in the following we will discuss three different scenarios for the transparency ratio T_A and CT :

1. no CT present; all hadrons in FSI interact with their full hadronic cross section from their creation vertex on

2. CT is only present in the hard partonic events which are determined by the underlying fragmentation model

3. both the hard partonic and soft diffractive events experience CT effect.

Throughout the following we shall also compare three different calculations:

1. calculations for a deuterium target including relative momenta of proton and neutron, including final state interactions (FSI) (albeit being a very small effect), are labeled by "D"

2. calculations for a nucleus, including Fermi motion and Pauli blocking, but no FSI (except particle decays) will be denoted by "A0" as e.g. "Fe0" for an Iron target

3. finally calculations on Iron as above, but now including the full FSI machinery are labeled by "Fe" (or in general by "A").

The calculations for finite nuclei are done here without the shadowing effect, expected to still be quite small at the energies and momenta relevant here. Since the coherence length has been kept nearly constant in the JLAB experiment the shadowing corrections are not effective in the Q^2 dependence of T_A.

IV. EXPERIMENTAL CUTS

Within the GiBUU transport model, one simulates the production of ρ^0 mesons (among others) on a Monte Carlo basis. All produced particles, independent of their production mechanism, are propagated through the nucleus according the transport equations. At the end we have four-vectors of all final state particles. This enables us to simulate all the experimental reconstruction of $\pi^+\pi^-$ events and cutting.

We start our considerations of acceptance conditions by looking at kinematics. In Figure 5 we show the accessible kinematical region in the ν-Q^2 plane for an electron beam energy $E_e = 5\,\mathrm{GeV}$. As can be seen there, the understanding of the acceptance in the region of small electron scattering angles is of major importance, since it influences strongly the possible minimal values of ν or W in the region of $Q^2 \lesssim 1\,\mathrm{GeV}^2$. Since effects of Fermi motion have most impact at low W, the variation in minimal W translates into the question, whether one observes them or not. In the following we will only use the acceptance cuts [29] for the scattered electron and assume full detection efficiency within these cuts ($\theta_e = 12^o \ldots 50^o$, $Q^2 > 0.6\,\mathrm{GeV}^2$).

In addition, the JLAB experiment [12] applies the cuts for the invariant mass W, the momentum transfer t and the incoming photon energy ν.

1. $W > 2\,\mathrm{GeV}$ in order to avoid the resonance region,

2. $t > -0.4\,\mathrm{GeV}^2$ to be in the diffractive region,

3. $t < -0.1\,\mathrm{GeV}^2$ to exclude coherent production off the nucleus,

4. $z = E_\rho/\nu > 0.9$ to select the elastic process; here E_ρ is the energy of the ρ^0 meson produced.

We note here, that the first cut relies on the assumption of a quasi-free process since the invariant mass W is calculated for a nucleon at rest, neglecting any Fermi motion. The actual minimal values for W for the elementary reaction to be considered in the calculations may, due to Fermi motion, reach much smaller values. Thus the first cut does not guarantee the desired region above the resonances.

The understanding of the second cut is of major importance for the interpretation of the high Q^2 part of the considered experiment. To see how the $t > -0.4\,\mathrm{GeV}^2$ cut acts in the (Q^2, ν) plane we now consider the kinematical limits for t in a collision on a nucleon at rest with $W^2 = M_N^2 - Q^2 + 2M_N\nu$. These are given by ($t_1 \le t \le t_0$)

$$t_{0,1} = \left(\frac{-Q^2 - m_\rho^2}{2W}\right)^2 - \left(\frac{2M_N\sqrt{\nu^2+Q^2} \mp \sqrt{(W^2+m_\rho^2-M_N^2)^2 - 4W^2m_\rho^2}}{2W}\right)^2 . \quad (3)$$

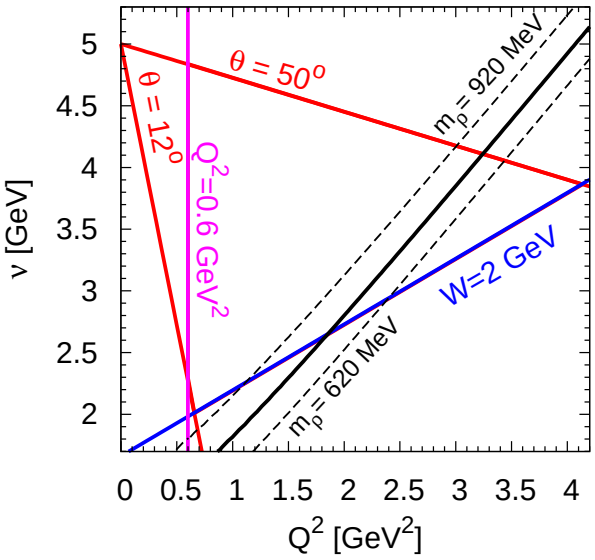

FIG. 5. (Color online) Experimental coverage in the ν–Q^2–plane corresponding to the electron beam energy $E_e = 5\,\mathrm{GeV}$. Lines correspond to the various cuts ($W > 2\,\mathrm{GeV}$, $Q^2 > 0.6\,\mathrm{GeV}^2$, $\theta_e > 12^o$ and $\theta_e < 50^o$). The upward sloping lines labeled by m_ρ indicate the cut at $t_0 = -0.4\,\mathrm{GeV}^2$ (solid) according eq. (3) with $m_\rho = 0.770\,\mathrm{GeV}$ and $m_\rho = 0.770 \pm 0.150\,\mathrm{GeV}$ (dashed curves). The rightmost curve corresponds to the smallest mass value. With this cut the region of large Q^2, to the right of the thick straight line, is forbidden for on-shell ρ production on a nucleon at rest.

where the notations for the variables are obvious. These purely kinematical limits for a nucleon at rest (or the deuterium target) directly translate into expressions for (Q^2, ν) at fixed $t_{0,1}$. The bound t_0, together with the experimental cut $t > -0.4\,\mathrm{GeV}^2$, translates also into a relation between ν and Q^2 and limits the values of Q^2 at fixed ν. This cut is shown in Figure 5 by the three parallel upward sloping lines. For the region of large Q^2 to the right of the lines on a nucleon (or deuterium) target no ρ^0 production with an on-shell mass is possible. However, the spectral function of the ρ^0 meson smears out this sharp cut. The two thinner dashed lines give a measure for the effects of the ρ^0 mass distribution.

For heavier nuclei all these considerations about the t cuts are smeared out further by Fermi motion. As a consequence, the cut is not so effective for such nuclei. We have indeed tested that with a realistic Fermi momentum distribution the cut on t_0 has no consequences for heavy nuclei, while it has a major effect for deuterium. As a consequence, any ratio of nuclear and nucleon (deuterium) cross sections will become very large in the large $Q^2 > 2.5\,\mathrm{GeV}^2$ region since there the denominator gets very small. This will be demonstrated in the following Section V.

Within our model we can not calculate coherent ρ^0 production off nuclei. We, therefore, apply the third cut as it is used in the data analysis. The fourth cut, however, is again accessible within our model. The exclusivity cut on high energies of the produced ρ is meant to enrich the ρ-CT signal and we apply it to our results.

As for the detection of the scattered electron, we will also assume full detection efficiency for the pions.

V. EFFECT OF FERMI MOTION

At first we demonstrate a trivial effect which can mimic the ρ-CT signal in the transparency ratio T_A. This effect is not generic and is merely tied to the special set of t kinematical cuts used in the actual JLAB experiment.

Since common to all hadronization models considered in the following we discuss first the effect of Fermi motion alone on the transparency ratio by analyzing the simplest ratio "A0/D0", i.e. the ratio of nuclear cross sections for some nucleus (without FSI) over calculations for deuterium (without FSI). In the final $\pi^+\pi^-$ Monte Carlo sample all the experimental cuts discussed above are taken into account. As one can see in Figure 6, for

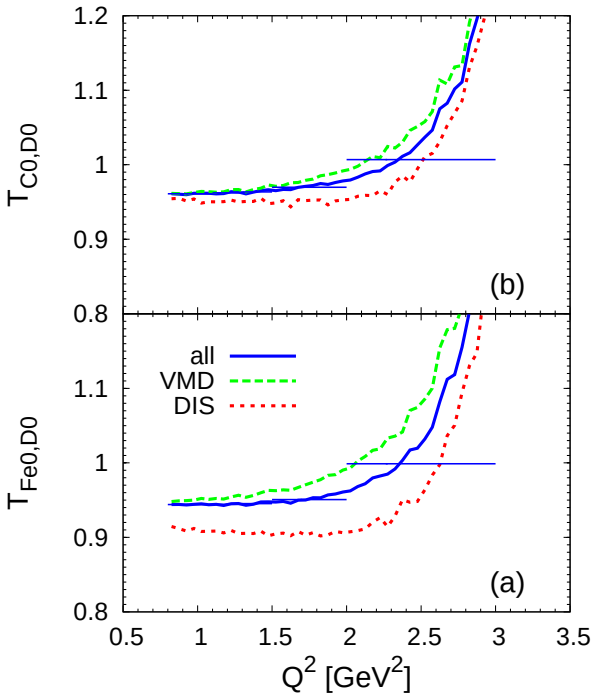

FIG. 6. (Color online) The transparency ratio for nuclei without FSI, i.e. the effect Fermi motion, for Fe (a) and C target (b). Only true ρ are used. The contributions of the processes are indicated by line style as 'all' (blue solid), 'VMD' (green dashed) and 'DIS' (red dotted). The thin horizontal lines repeat the results for 'all', but now with a coarse binning in Q^2.

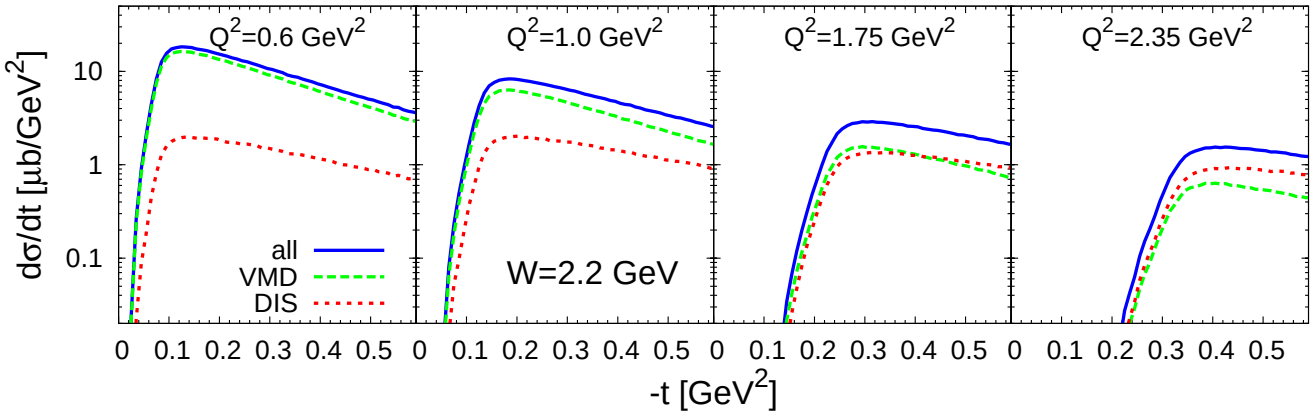

FIG. 7. (Color online) Differential cross section $d\sigma/dt$ in the reaction $p(\gamma^*, \rho)p$ for different values of Q^2 and a value of $W = 2.2\,\mathrm{GeV}$ in the kinematics of JLAB experiment. The solid curves are the sum of VMD (dashed) and DIS (dotted) contributions.

both ^{12}C/D and ^{56}Fe/D ratios we observe that this transparency ratio rises sharply to values above 1 for Q^2 values larger than $\simeq 2.5\,\mathrm{GeV}^2$ following – at smaller Q^2 – that of the VMD component, which is dominant here. This increase is a consequence of Fermi motion alone, since all FSI are turned off. This artificial rise of T_A for $Q^2 > 2.5\,\mathrm{GeV}^2$ is due to the t-cut discussed in Section IV that influences the denominator (the cross section off the deuterium target) in the transparency ratio much more strongly than the numerator. In Figure 6 we also show the results obtained when a coarse binning in Q^2 similar to that in the experiment is applied. In this case the rise of the curves is not so visible anymore. However, a bin expanding from $Q^2 = 2\,\mathrm{GeV}^2$ to $Q^2 = 3\,\mathrm{GeV}^2$ is still clearly affected.

Thus, Fermi motion alone can mimic a behavior with Q^2 that is qualitatively expected for CT. At lower values of Q^2 the rise of T_A shows up only in the VMD and not in the DIS component. This is due to the fact that the partonic DIS events are more isotropically distributed, whereas the diffractive events are forward peaked. Then the t-cut is not so effective.

The forward differential cross sections $d\sigma/dt$ at $W = 2.2\,\mathrm{GeV}$ and for different values of Q^2 bins are shown in Figure 7. Different slopes of different ρ^0 production components can be clearly seen. In the kinematics of the JLAB experiment the low Q^2 region is dominated by the diffractive VMD component. On the contrary, the high Q^2 region is partonic.

Figure 6 also shows that $T_A < 1$ for $Q^2 < 2.5\,\mathrm{GeV}^2$. This lowering of T_A even in the absence of any FSI is again due the experimental t-cut described above.

Note that, the effects of Fermi motion on the transparency could be minimized by normalizing the transparency ratio T_A to the ^{12}C cross section.

VI. RESULTS ON TRANSPARENCY

A. No CT

The transparency for the model in which all created hadrons interact with their full hadronic cross section from their point of creation on is shown in Figure 8. It is seen that the transparency – as in the case with Fermi motion only – increases only weakly until $Q^2 \approx 2\,\mathrm{GeV}^2$ and then rises steeply for larger Q^2. This latter strong rise is – as already discussed – due to the t-cut and is present even for the case of Fermi motion alone, see Figure 6.

It is worthwhile to separate our results into their origins and to look at the question, whether VMD or DIS induced ρ^0 are attenuated differently. Therefore we show in Figure 8 the results separately for DIS and VMD ρ^0s. While both the VMD and the DIS parts noticeably increase with Q^2 the resulting total curve is flatter than the

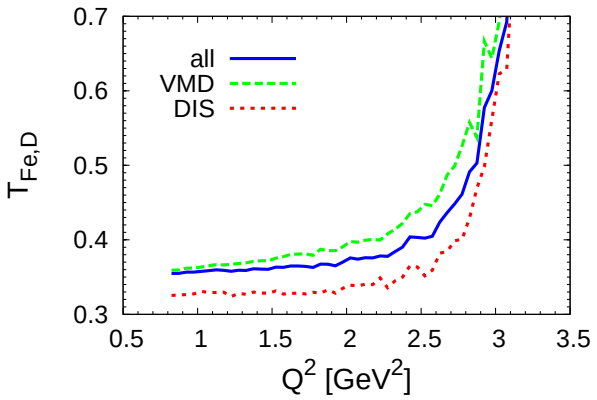

FIG. 8. (Color online) The transparency ratio of ρ^0 for Fe target in the scenario without CT. The contributions of the processes are indicated by line style as 'all' (blue solid), 'VMD' (green dashed) and 'DIS' (red dotted).

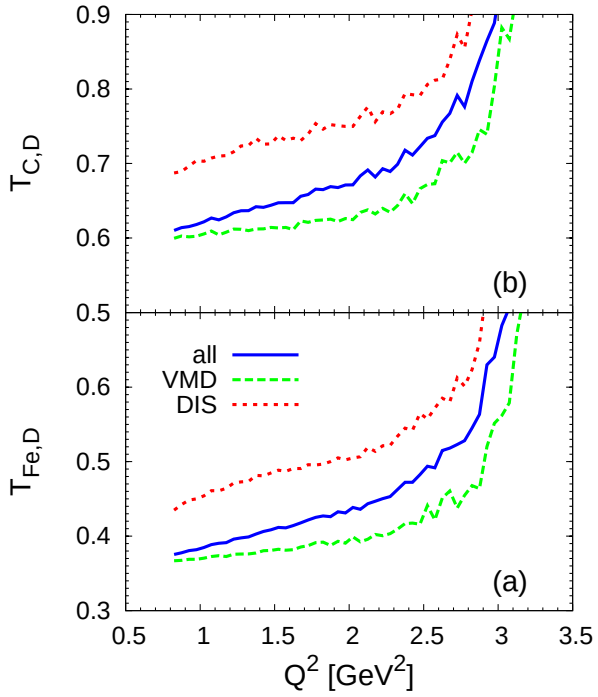

FIG. 9. (Color online) The transparency ratio of ρ^0 for Fe (a) and C (b) target in the scenario, where only the DIS part has CT effects. The contributions of the processes are indicated by line style as 'all' (blue solid), 'VMD' (green dashed) and 'DIS' (red dotted).

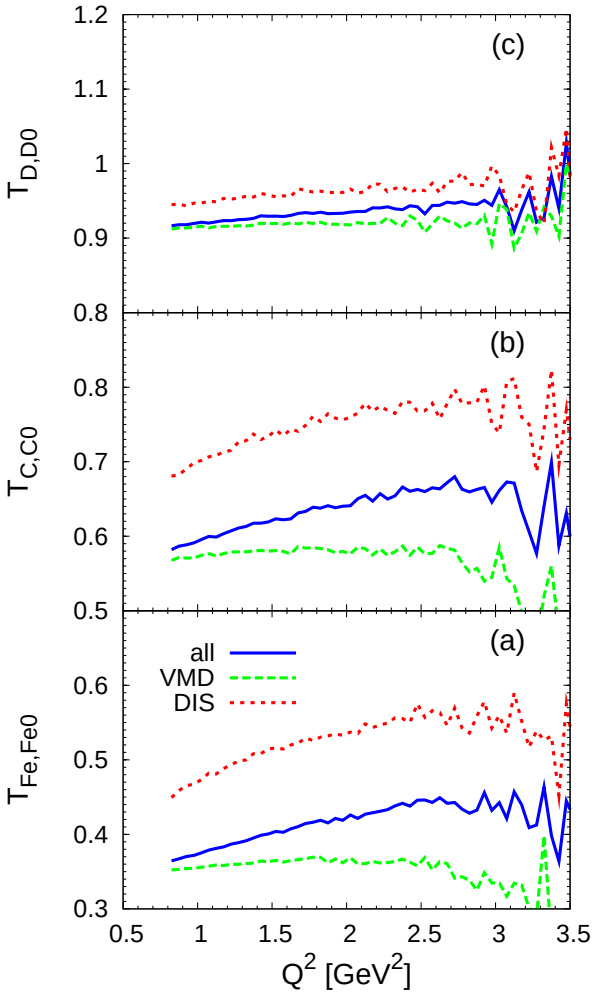

FIG. 10. (Color online) The ratio of all ρ^0s produced on ^{56}Fe (a), ^{12}C (b) and D (c) to that on the same targets, respectively, but without FSI. The contributions of the processes are indicated by line style as 'all' (blue solid), 'VMD' (green dashed) and 'DIS' (red dotted).

VMD contribution because with increasing Q^2 also the weight of DIS events increases. Since these DIS events are more strongly attenuated the transparency T_A is being held down until the t-cut effects prevail.

B. CT only for DIS events

We turn now to the discussion of the CT only for hard DIS events. In the previous considerations we have assumed that all particles interact immediately after their creation with their full cross section, i.e. that there are no CT effects at work. In earlier work we have shown that this assumption does not hold for higher beam energies [28] or for exclusive pion production at CLAS energies[14]. Therefore we now use a hadronization picture as developed in [27, 28]. In this picture the hadronic interactions cross section in FSI grows linearly with time [5], see Eq. (2). The expansion time τ_f, which we identify with the formation time in the definition of [27], is obtained from the string breaking mechanism as outlined in [27]. On the other hand, the ρ^0 from diffractive VMD events are assumed to start interacting with their full hadronic cross section immediately after their production.

In Figure 9 we show the result on the hadron attenuation. The rise of the VMD component is the same as that in Fig. 8 and is entirely caused by the Fermi motion. It dominates T_A at small Q^2. At large Q^2 we find a stronger increase with Q^2 compared to the case without CT, driven by the weakened interaction of the DIS-like events during the expansion time. The ρ^0s stemming from DIS events are less attenuated, while the ρ^0 from VMD events are unaffected (as expected). Since in the final ratio we have an admixture of both origins such that the weight of DIS events increases with Q^2 also the overall transparency increases with Q^2 in this scenario. In the scenario without CT effect, see Figure 8, the partonic DIS contribution is more strongly attenuated than the VMD part and there the mixing has an opposite effect.

In order to separate the effects of CT from those originating in the Fermi motion we show in Figure 10 the ratio of the ρ^0 production on D, ^{12}C and ^{56}Fe to that on the same targets, respectively, without any FSI. The

rise of the DIS component of the transparency in Fig. 10 with Q^2 is due to the $1/Q^2$-dependence of the first term in Eq. 2. We note, however, that already for a deuterium target, the FSI introduce an effect in the order of 5-10%.

C. CT for DIS and VMD events

In a next step, in order to study the CT effects also for VMD events, we assume in a third model that all ρ^0 have a finite formation time $t_F = \gamma\tau_F$ in the laboratory. Here γ is the Lorentz boost factor, while the formation time in the rest frame of the ρ^0 is taken to be $\tau_F = 0.4\,\mathrm{fm}$, the value used in [13][2]

In this last extreme picture, see Figure 11, one observes a strong increase of the attenuation ratio with Q^2. It is essentially the same for both VMD and DIS components.

The final results in Fig. 11 show a very steep rise of T_A with Q^2 which seems to be ruled out by the preliminary experimental data. However, before jumping to such conclusions we recall that the final result depends on a number of ingredients, which all conspire with each other in affecting the observable transparency. Among them is – foremost – the Fermi-motion and its interplay with the experimental t-cuts. The influence of the latter also varies with the t-dependence of the experimental cross section.

We also note that a large part of the observed ρ^0 suppression is due to pion reabsorption in FSI. This then raises interesting, but hard to answer questions on the ρ^0 decay during its expansion time and on the inclusion of CT effects for pions from ρ^0 decay. The pion FSI then complicate any experimental determination of CT for the ρ meson.

VII. CONCLUSIONS

In this paper we have investigated the effects of various experimental (cuts) and theoretical (Fermi-motion) properties on an experiment aiming for a verification of color transparency at JLAB energies. We have illustrated that a careful analysis of experimental acceptances and cuts can have an influence on the final results because these cuts tend to include different kinematical regions in the numerator and the denominator of the transparency ratio. As a consequence, the elementary production cross sections do not drop out in the transparency ratio, but have to be explicitly taken into account. The observed transparency is then no longer a measure for FSI alone, but is also affected by all these effects just mentioned.

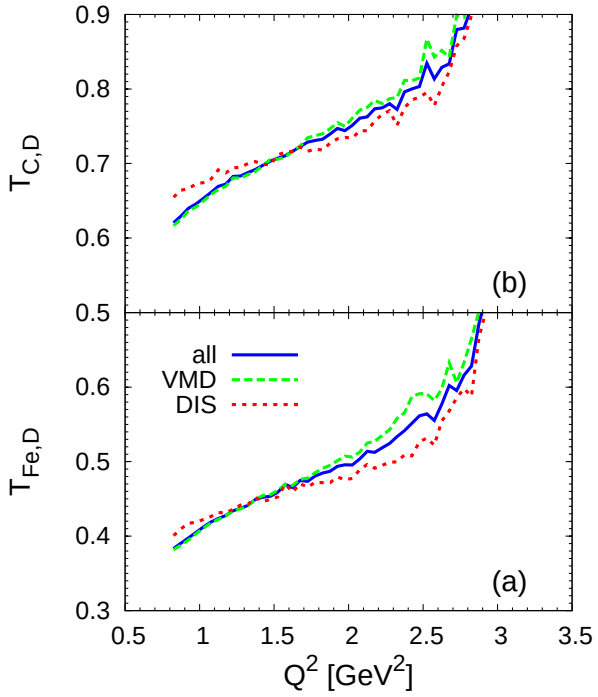

FIG. 11. (Color online) The transparency ratio of ρ^0 for ^{56}Fe (a) and ^{12}C (b) target in a scenario where all the produced ρ experience the CT effect. The contributions of the processes are indicated by line style as 'all' (blue solid), 'VMD' (green dashed) and 'DIS' (red dotted).

This has consequences, for example, for the interpretation of a recent experiment at JLAB on nearly-exclusive ρ^0 production.

We have also shown that in this experiment different event types (VMD and DIS) contribute significantly in different Q^2 ranges and – due to their different absorption – can affect the behavior of the transparency. Furthermore, Fermi motion can smear the W and t ranges and, as a consequence, leads to a strong rise of the transparency with Q^2 at large momentum transfers. This latter behavior is always there and has to be separated from the rise of T_A with Q^2 expected from CT.

Our calculations show that in the range of smaller values of $Q^2 < 2.2\,\mathrm{GeV}^2$ CT indeed leads to a larger rise than that given by Fermi motion alone. The rise – above that expected from Fermi motion alone – is directly proportional to the expansion time. It could thus be possible to determine the latter from a careful analysis of the data.

A complementary experimental proposal for the future JLAB facilities would be to measure the transparency ratio and ρ-CT in the decay of ρ^0 into dilepton e^+e^- pairs, thus continuing the successful g7 experiment that worked with real photons [30]. This could provide much cleaner sample of events which are not contaminated by the in-medium FSI of pions as in the hadronic $\rho \to \pi^+\pi^-$ reconstruction experiments.

[2] The string-expansion times extracted from PYTHIA, which were used in scenario 2, are on average larger by about a factor of 2. This observation is important because the (not well-known) expansion time has a crucial influence on absolute height and the slope of T_A as a function of Q^2.

ACKNOWLEDGMENTS

The authors thank Kawtar Hafidi and Lamia El Fassi for their patience explaining to us their detector and experimental procedures. We gratefully acknowledge helpful discussions with the whole GiBUU group. We also gratefully acknowledge support by the Frankfurt Center for Scientific Computing, where parts of the calculations were performed. This work was supported by the HIC for FAIR, by BMBF and by DFG under SFB/TR16.

[1] S. J. Brodsky and A. H. Mueller, Phys. Lett. B **206**, 685 (1988)
[2] L. Frankfurt, G. A. Miller and M. Strikman, Comments Nucl. Part. Phys. **21**, 1 (1992).
[3] P. Jain, B. Pire and J. P. Ralston, Phys. Rept. **271**, 67 (1996).
[4] B. K. Jennings and G. A. Miller, Phys. Lett. **B274**, 442 (1992).
[5] G. R. Farrar, H. Liu, L. L. Frankfurt and M. I. Strikman, Phys. Rev. Lett. **61**, 686 (1988).
[6] A. Airapetian *et al.*, Phys. Rev. Lett. **90**, 052501 (2003).
[7] J. L. S. Aclander *et al.*, Phys. Rev. C **70**, 015208 (2004).
[8] A. S. Carroll *et al.*, Phys. Rev. Lett. **61**, 1698 (1988).
[9] M. R. Adams *et al.*, Phys. Rev. Lett. **74**, 1525 (1995).
[10] T. Falter, K. Gallmeister and U. Mosel, Phys. Rev. **C67**, 054606 (2003).
[11] B. Z. Kopeliovich, J. Nemchik, A. Schafer and A. V. Tarasov, Phys. Rev. **C65**, 035201 (2002).
[12] CLAS, K. Hafidi *et al.*, in preparation.
[13] L. Frankfurt, G. A. Miller and M. Strikman, Phys. Rev. **C78**, 015208 (2008).
[14] M. M. Kaskulov, K. Gallmeister and U. Mosel, Phys. Rev. C **79**, 015207 (2009).
[15] B. Clasie *et al.*, Phys. Rev. Lett. **99**, 242502 (2007).
[16] W. Cosyn, M. C. Martinez and J. Ryckebusch, Phys. Rev. C **77**, 034602 (2008).
[17] A. Larson, G. A. Miller and M. Strikman, Phys. Rev. C **74**, 018201 (2006).
[18] M. M. Kaskulov, K. Gallmeister and U. Mosel, Phys. Rev. D **78**, 114022 (2008).
[19] M. M. Kaskulov and U. Mosel, Phys. Rev. C **80**, 028202 (2009).
[20] M. M. Kaskulov and U. Mosel, Phys. Rev. C **81**, 045202 (2010).
[21] I. T. Obukhovsky *et al.*, Phys. Rev. D **81**, 013007 (2010).
[22] J. D. Bjorken and J. Kogut, Phys. Rev. D **8**, 1341 (1973).
[23] S. A. Morrow *et al.* [CLAS Collaboration], Eur. Phys. J. A **39**, 5 (2009)
[24] GiBUU homepage, http://gibuu.physik.uni-giessen.de
[25] B. Z. Kopeliovich, J. Nemchick, N. N. Nikolaev and B. G. Zakharov, Phys. Lett. B **324**, 469 (1994).
[26] B. Z. Kopeliovich, J. Nemchick, N. N. Nikolaev and B. G. Zakharov, Phys. Lett. B **309**, 179 (1993) [arXiv:hep-ph/9305225].
[27] K. Gallmeister and T. Falter, Phys. Lett. **B630**, 40 (2005).
[28] K. Gallmeister and U. Mosel, Nucl. Phys. **A801**, 68 (2008).
[29] K. Hafidi, L. El Fassi, private communication.
[30] M. H. Wood *et al.* [CLAS Collaboration], Phys. Rev. **C78**, 015201 (2008).